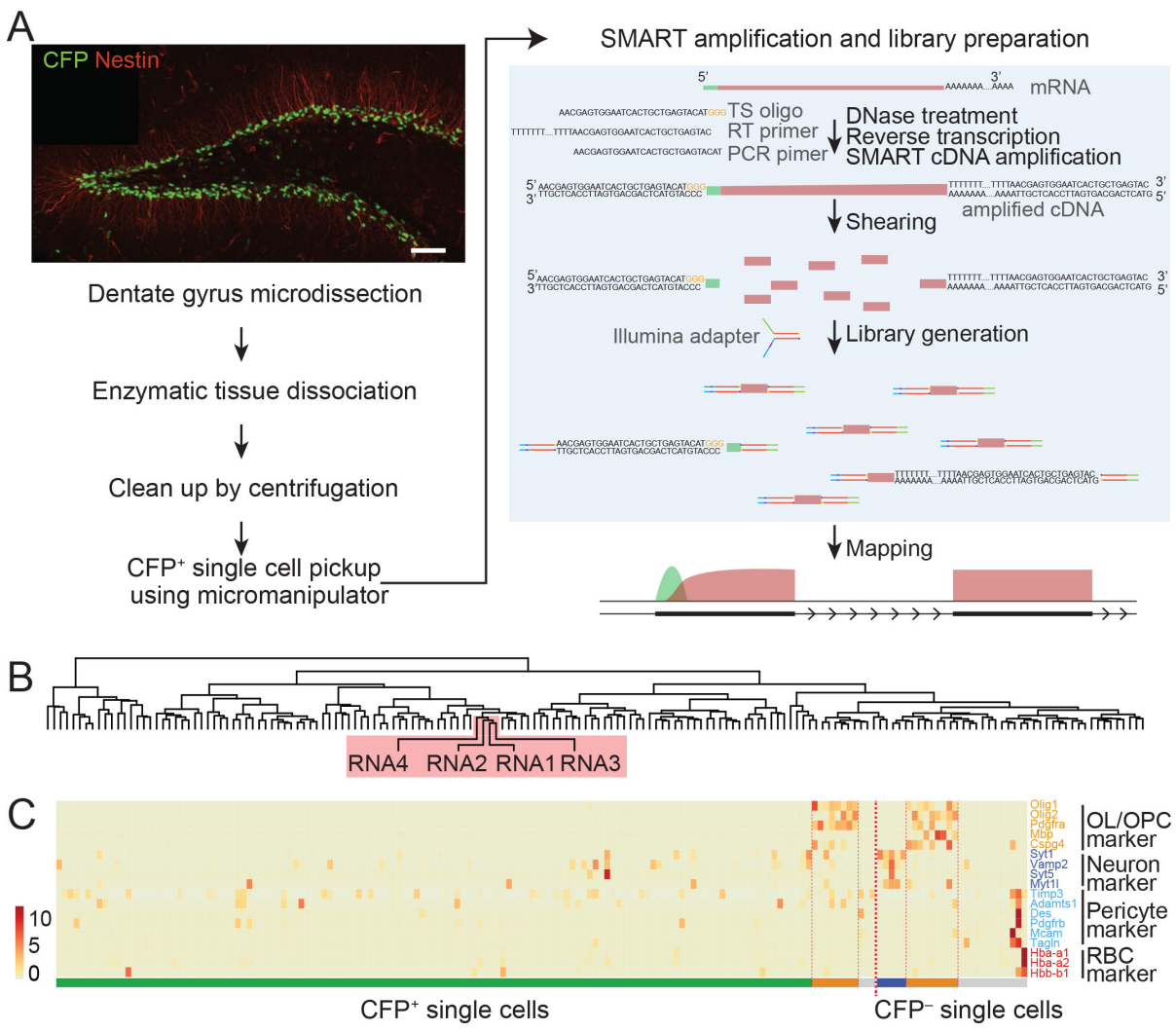


**Figure S1. Single-cell RNA-seq of labeled precursor cells from the adult mouse dentate gyrus, related to Figure 1.**

(A) A schematic diagram of experimental procedures for achieving single-cell transcriptomes from fluorescently labeled individual cells isolated from the adult *Nestin-CFP$^{nuc}$* mouse dentate gyrus. Shown at the top is a sample confocal image of *Nestin-CFP$^{nuc}$* adult mouse dentate gyrus for CFP and Nestin immunostaining. Scale bar: 100 μm. Isolation of individual NPCs involved the following steps: (1) microdissection of tissues of interest; (2) dissociation of tissue using papain and DNase I; (3) eliminating cell debris via multiple rounds of mild centrifugation; and (4) picking up fluorescently labeled individual cells using a micromanipulator with a pulled glass micropipette and breaking the tip of the glass pipette into PCR strips. The SMART amplification protocol (Ramskold et al., 2012) was followed with minor modifications, including DNase I digestion before adding polyT primer. Library generation followed conventional Illumina library preparation protocol after fragmentining the amplified cDNA. TS oligo: Template Switch oligo; RT primer: primer for reverse transcription; SMART: Switching Mechanism At 5' end of RNA Template.

(B) Unsupervised clustering for individual CFP$^+$ and CFP$^-$ cells, and single-cell equivalent amount (3 pg) of whole-dentate gyrus RNA samples (n = 4). Whole dentate RNA samples are highlighted to show the extensive biological variability of single-cell transcriptomes, compared to negligible technical variability.

(C) Expression heat map of known markers for oligodendrocyte precursor cells (OPC)/oligodendrocytes (OL), pericytes, and blood cells. Horizontal bar under the heat map represents putative cell types determined by marker expression profiles. Green: cells with potential NPC lineages; Orange: cells with OPC/OL lineages; Purple: cells with differentiated neuronal characteristics; Gray: uncharacterized outliers or cells with non-neuronal lineages.

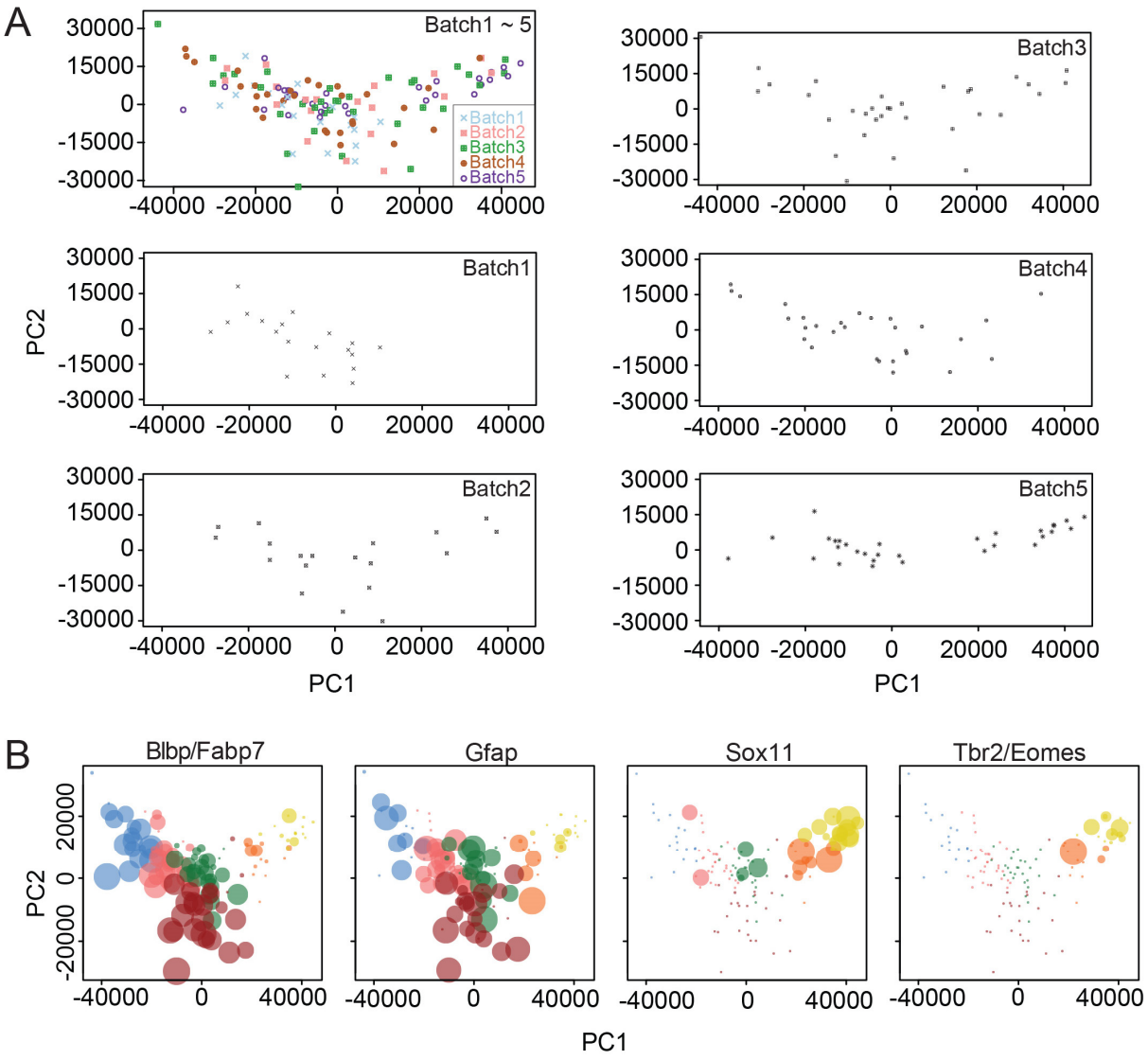


**Figure S2. Reproducibility and orientation of the developmental trajectory on the PCA plot, related to Figure 2.**

(A) Shown are PCA plots with all Nestin-CFP$^{nuc+}$ NPCs (top left panel) and with Nestin-CFP$^{nuc+}$ NPCs in five individual sequencing runs.

(B) Normalized expression levels of known marker genes on the PCA plot, represented by the size of data points. Colors of data points follow the color codes in Figure 2B. Notably, known NSC markers Blbp/Fabp7 and Gfap were highly expressed on the left side, whereas eIPC markers Tbr2/Eomes and Sox11 were highly expressed on the right side.

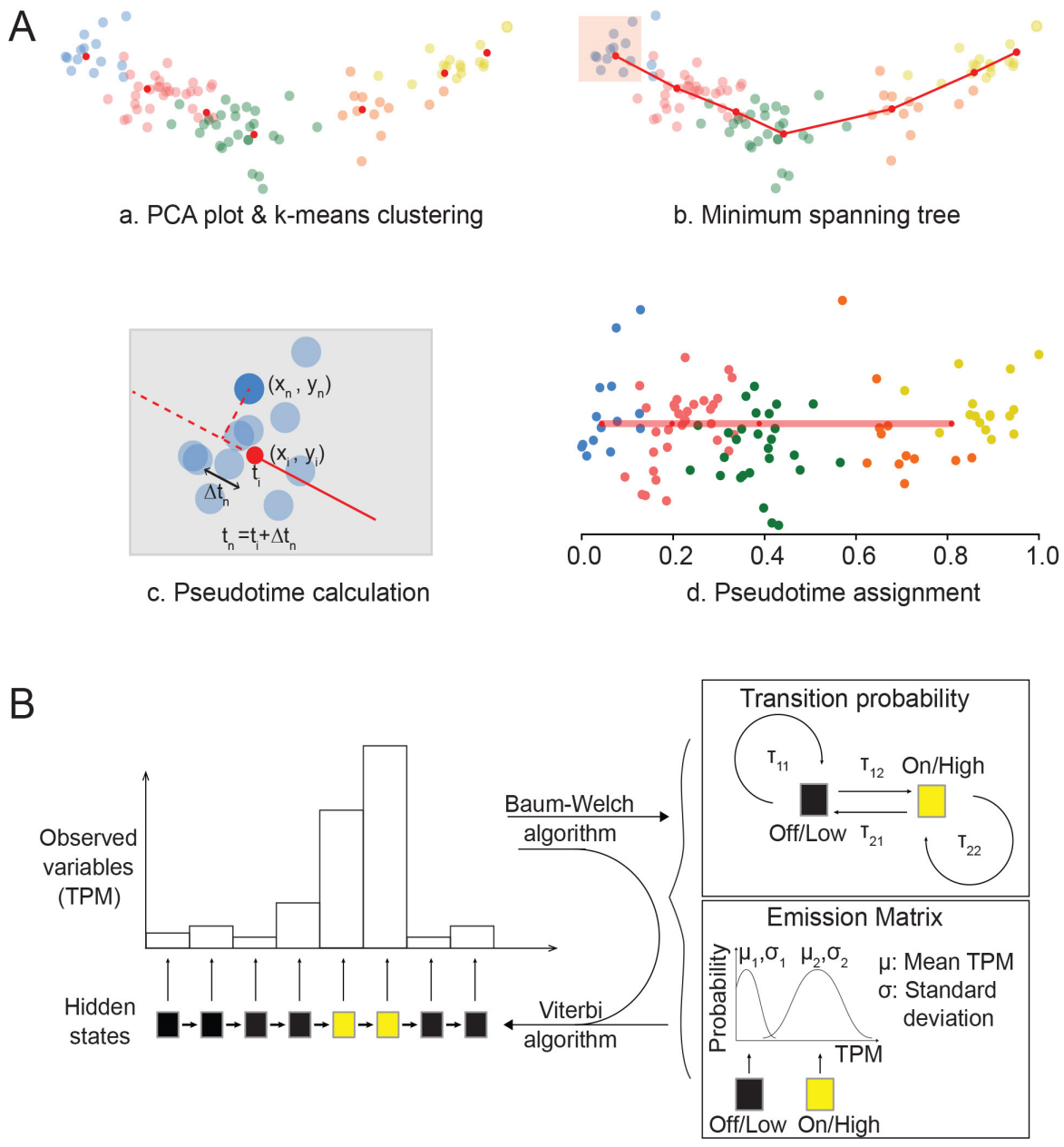


**Figure S3. Waterfall algorithms, related to Figure 2.**
(A) An illustration of steps to generate an averaged trajectory and assign pseudotime to each individual cell: (a) Representing individual cells on the PCA plot with PC1 and PC2 and performing k-means from the PCA data (small red dots); (b) Building a trajectory connecting k-means as minimum spanning trees (MST); (c) Determining the relative location of each cell using orthogonal line to connect each cell to the closest trajectory line; (d) Assigning pseudotime for each cell based on its relative location on the trajectory.
(B) An illustration of the approach to predict underlying states from gene expression (TPM) over pseudotime progression. The Baum-Welch algorithm predicts the most likely transition probability and emission matrix from observed variables (TPM). The Viterbi algorithm uses observed variables (TPM) along with the output from the Baum-Welch algorithm to predict hidden On/High and Off/Low gene expression states.

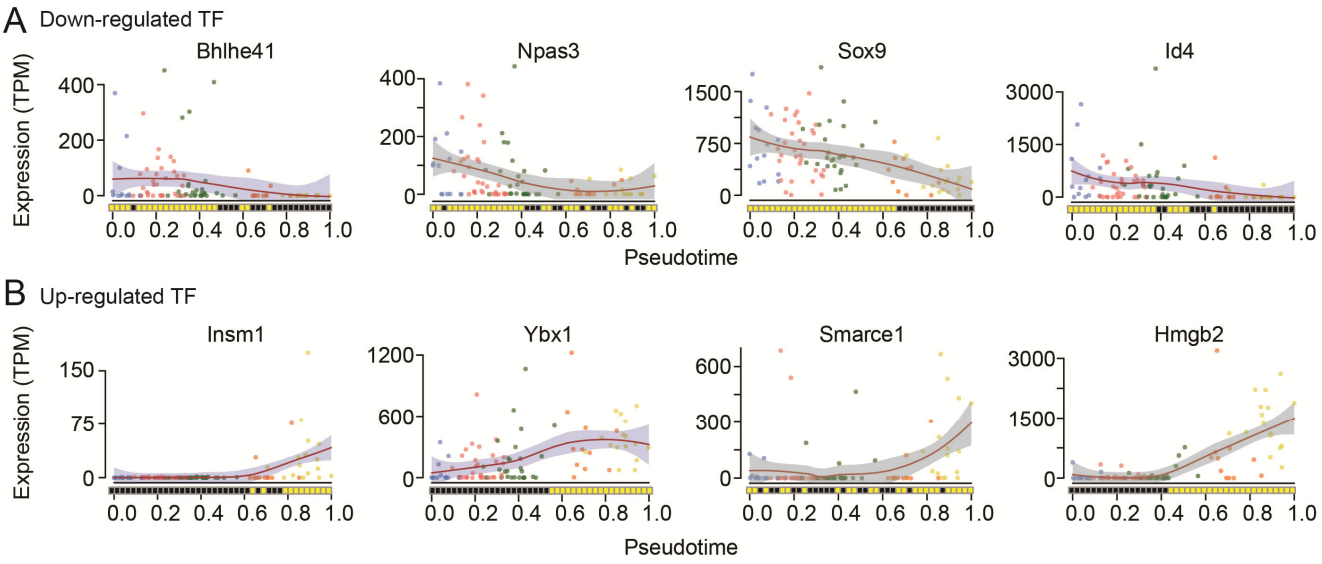


**Figure S4. Pseudotime profiles of sample transcription factors, related to Figure 4.**
Shown are pseudotime profiles of representative transcription factors that were down-regulated (A) or up-regulated (B) over developmental pseudotime progression. Similarly plotted as in Figure 2D.

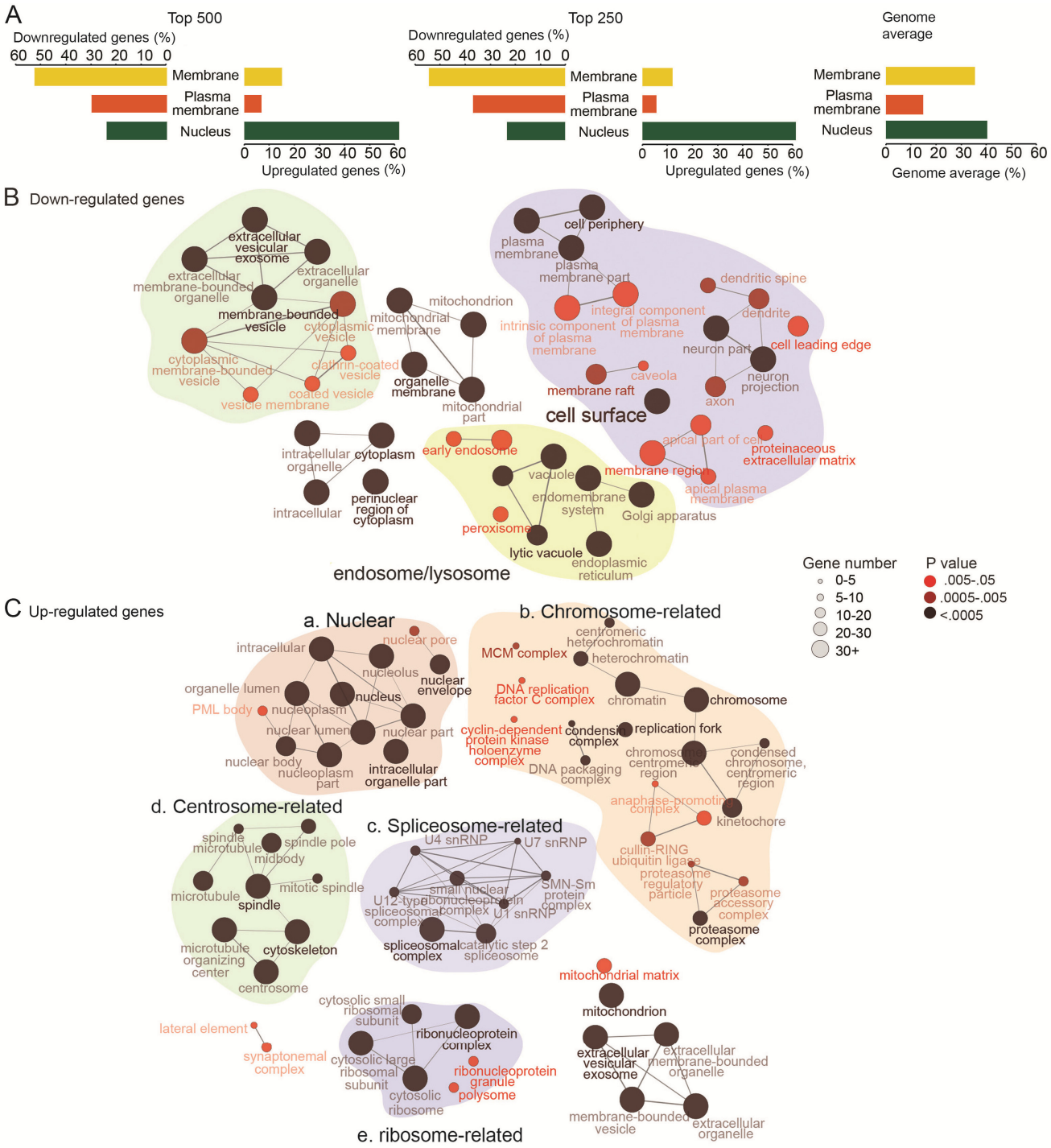


**Figure S5. Cellular compartment analysis for UP and DOWN genes, related to Figure 5.**
(A) Cellular compartment analysis for UP and DOWN genes with different thresholds. Shown are summaries of enrichment patterns of UP and DOWN genes with cutoff for top 500 genes (left panel) or top 250 genes (middle panel), and average for all genes (right panel).
(B-C) Detailed predicted cellular locations for gene products of DOWN$^{1000}$ genes (B) and of UP$^{1000}$ genes (C). The size of each data point represents the number of genes within each predicted location, and color of each data point represents P value of enrichment to each predicted location. P values are from hypergeometric test and corrected by Holm–Bonferroni method (Bonferroni step-

down correction). Connections between pairs of data points represent sharing more than 50% of genes between the pair. Similar entities are grouped with the same background colors.

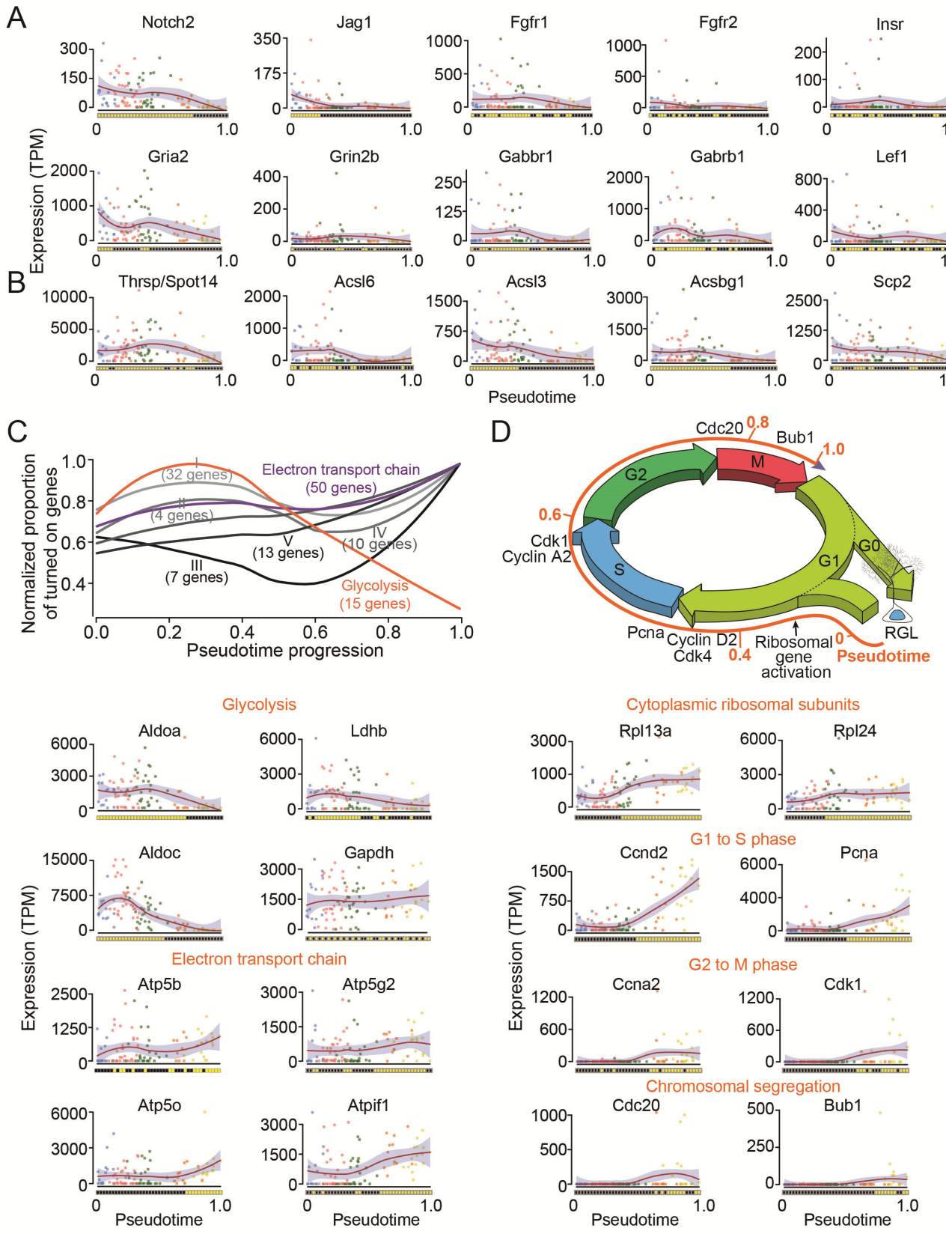


**Figure S6. Representative pseudotime profiles of key genes related to niche signaling, cell cycle progression, and energy metabolism, related to Figures 6 & 7.**

(A-B) Pseudotime profiles of representative genes related to niche signaling (A) and genes related to fatty acid metabolism (B), both of which exhibited down-regulation upon qNSC activation. Similarly plotted as in Figure 2D.
(C) Reciprocal changes of expression of mitochondrial electron transport genes and glycolysis genes. Roman numerals represent electron transport complex. Complex V exhibited a clear increase throughout early neurogenic pseudotime. Shown at the bottom are pseudotime profiles of some genes related to glycolysis (gradual down-regulation) and complex V genes in mitochondrial electron transport chain (gradual up-regulation).
(D) Developmental pseudotime recapitulates cell cycle progression during qNSC activation and initiation of neurogenesis. Shown on the top is a schematic illustration of cell cycle phases correlated with pseudotime. Cell cycle checkpoint genes were up-regulated following the sequence of biological cell cycle progression. Shown at the bottom are pseudotime profiles of genes related to cell cycle checkpoints and cytoplasmic ribosomal subunits. Note that ribosomal genes were up-regulated earlier than any of the cell cycle related genes.

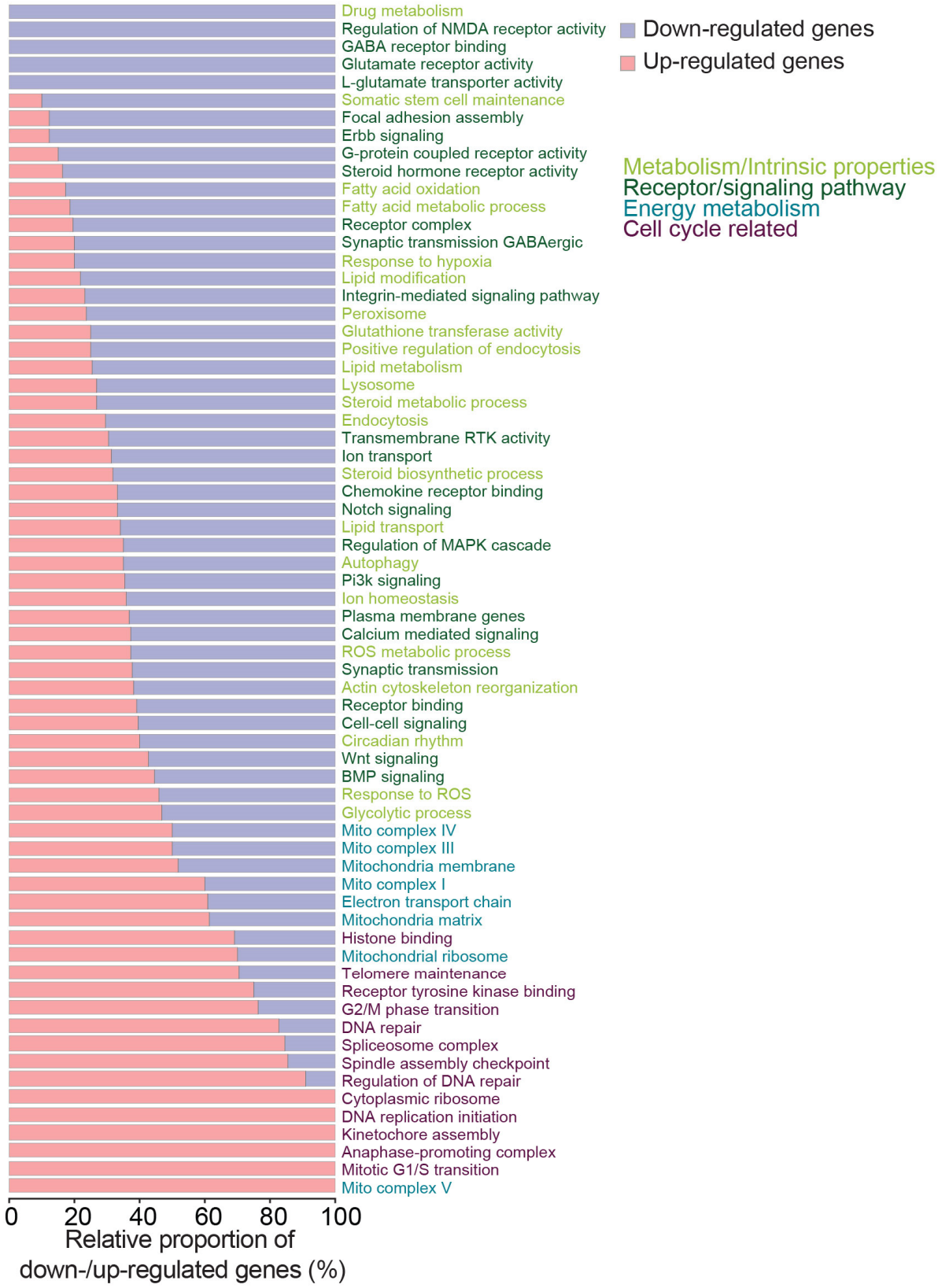


**Figure S7. Independent validation for GO entity enrichment test for up-regulated and down-regulated genes during quiescent stem cell activation and neurogenesis, related to Figures**

**5 & 6.**
Shown is a summary of the proportion of up-regulated and down-regulated genes within each key functional GO entity. GO entities with a disproportionally higher proportion of up-regulated genes represent functional pathways that are activated during exit of quiescence and early stages of neurogenesis, whereas GO entities with a disproportionally higher proportion of down-regulated genes represent functional pathways that are qNSC-specific pathways.

**Supplementary Tables**

**Table S1.** Summary of sequencing statistics, **related to Figure 1.**

**Table S2.** List of literatures consistent with the predicted molecular dynamics of adult neural stem cell, **related to all figures.**

**Table S3.** Adult NPC-enriched gene list and validation based on the Allen Brain in situ database, **related to Figure 1.**

**Table S4.** 1000 UP genes and 1000 DOWN genes and their Spearman correlation coefficient to pseudotime, **related to Figure 4.**

**Table S5.** List of UP TFs and DOWN TFs, **related to Figure 4**.

**Table S6.** Single-cell gene expression table according to the pseudotime progression, **related to Figure 5.**

**Table S7.** Three groups of genes based on their correlation with pseudotime, **related to Figure 5.**

**Supplementary Data**

This zipped file contains R codes to run Waterfall for datasets in the main text and in the Supplementary Methods, a README text file, and a PDF file for the Supplementary Methods and references.